Available online at www.sciencedirect.com

ScienceDirect

Nuclear Physics B 893 (2015) 89–106

NUCLEAR PHYSICS B

www.elsevier.com/locate/nuclphysb

Renormalization group evolution of neutrino parameters in presence of seesaw threshold effects and Majorana phases

Shivani Gupta [a], Sin Kyu Kang [b], C.S. Kim [a,*]

[a] *Department of Physics and IPAP, Yonsei University, Seoul 120-749, Republic of Korea*
[b] *School of Liberal Arts, Seoul-Tech, Seoul 139-743, Republic of Korea*

Received 8 July 2014; received in revised form 26 January 2015; accepted 28 January 2015

Available online 4 February 2015

Editor: Tommy Ohlsson

Abstract

We examine the renormalization group evolution (RGE) for different mixing scenarios in the presence of seesaw threshold effects from high energy scale (GUT) to the low electroweak (EW) scale in the Standard Model (SM) and Minimal Supersymmetric Standard Model (MSSM). We consider four mixing scenarios namely Tri–Bimaximal Mixing, Bimaximal Mixing, Hexagonal Mixing and Golden Ratio Mixing which come from different flavor symmetries at the GUT scale. We find that the Majorana phases play an important role in the RGE running of these mixing patterns along with the seesaw threshold corrections. We present a comparative study of the RGE of all these mixing scenarios both with and without Majorana CP phases when seesaw threshold corrections are taken into consideration. We find that in the absence of these Majorana phases both the RGE running and seesaw effects may lead to $\theta_{13} < 5^\circ$ at low energies both in the SM and MSSM. However, if the Majorana phases are incorporated into the mixing matrix the running can be enhanced both in the SM and MSSM. Even by incorporating non-zero Majorana CP phases in the SM, we do not get θ_{13} in its present 3σ range. The current values of the two mass squared differences and mixing angles including θ_{13} can be produced in the MSSM case with $\tan\beta = 10$ and non-zero Majorana CP phases at low energy. We also calculate the order of effective Majorana mass and Jarlskog Invariant for each scenario under consideration.

* Corresponding author.
E-mail addresses: shivani@yonsei.ac.kr (S. Gupta), skkang@seoultech.ac.kr (S.K. Kang), cskim@yonsei.ac.kr (C.S. Kim).

http://dx.doi.org/10.1016/j.nuclphysb.2015.01.026

Table 1
Experimental constraints on neutrino mass squared differences and mixing angles [7].

Parameter	Best fit	3σ range
$\Delta m^2_{12}/10^{-5}$ eV^2	7.50	7.00–8.09
$\Delta m^2_{13}/10^{-3}$ eV^2	2.473	2.276–2.695
θ°_{12}	33.36	31.09–35.89
θ°_{13}	8.66	7.19–9.96
θ°_{23}	40.0, 50.4	35.8–54.8

1. Introduction

Many flavor symmetries studied in literature [1,2] can result in some particular form of mixing in leptonic sector. The mixing scenarios obtained by some symmetries lead to the vanishing reactor neutrino mixing angle, θ_{13}. However, non-zero θ_{13} has been measured by the reactor experiments [3], it is meaningful to turn to systematic study of the effects of perturbation on flavor symmetries or to search for alternative symmetry which gives non-zero θ_{13}. In the flavor basis leptonic mixing matrix is given as

$$U = \begin{pmatrix} c_{12}c_{13} & s_{12}c_{13} & s_{13}e^{-i\delta_{CP}} \\ -s_{12}c_{23} - c_{12}s_{23}s_{13}e^{i\delta_{CP}} & c_{12}c_{23} - s_{12}s_{23}s_{13}e^{i\delta_{CP}} & s_{23}c_{13} \\ s_{12}s_{23} - c_{12}c_{23}s_{13}e^{i\delta_{CP}} & -c_{12}s_{23} - s_{12}c_{23}s_{13}e^{i\delta_{CP}} & c_{23}c_{13} \end{pmatrix} \cdot P. \tag{1.1}$$

Here $c_{ij} = \cos\theta_{ij}$, $s_{ij} = \sin\theta_{ij}$; θ_{ij} are the three mixing angles, δ_{CP} is the Dirac CP phase. The matrix $P = Diag(1, e^{-i\varphi_1/2}, e^{-i\varphi_2/2})$ has two Majorana CP phases φ_1 and φ_2 respectively. The relatively large value of θ_{13} has also provided an opportunity to measure δ_{CP} in the lepton mixing matrix. The Jarlskog rephasing invariant quantity, J_{CP} given as $J_{CP} = c_{12}s_{12}c_{23}s_{23}c^2_{13}s_{13}\sin\delta_{CP}$ [4] controls the magnitude of CP violation in neutrino oscillations generated by δ_{CP}. Recent global fit analysis for the neutrino parameters is given in [5–7]. The best fit values along with the 3σ constraints on neutrino mass squared differences and mixing angles are given in Table 1. The mixing in neutrino sector is still not completely understood. We do not know whether the hierarchy of three neutrino masses is normal ($m_1 < m_2 < m_3$) or inverted ($m_3 < m_1 < m_2$). The CP violating phases are totally unknown at present. The absolute mass scale of neutrinos is still not known. The possible measurement of effective Majorana mass in neutrinoless double beta decay experiments will provide an additional constraint on the neutrino mass scale and Majorana CP phases. The effective Majorana mass can be expressed as

$$M_{ee} = |m_1c^2_{12}c^2_{13} + m_2s^2_{12}c^2_{13}e^{-i\varphi_1} + m_3s^2_{13}e^{-i(2\delta_{CP}+\varphi_2)}|. \tag{1.2}$$

The Planck Collaboration [8] has given the cosmological constraint on the sum of neutrino masses to be $\Sigma m_{\nu_i} < 0.23$ eV at 95% C.L. This sum of neutrino masses depend on values chosen for the priors and can be in the range (0.23–0.933) eV. The bounds and limits are needed to be tested in the forthcoming observations.

The fact that θ_{13} is not only non zero but relatively large motivates us to study how well the flavor symmetries can predict zero value of θ_{13}. Some of the mixing scenarios from flavor symmetries are Tri–Bimaximal Mixing (TBM) [9], Bimaximal Mixing (BM) [10], Hexagonal Mixing (HM) [11] and Golden Ratio (GR) [2,12]. All these mixing scenarios predict the vanishing θ_{13} and maximal atmospheric mixing angle i.e. $\theta_{23} = \pi/4$. The solar mixing angle θ_{12} is

Table 2
The mixing matrices U and their corresponding light neutrino mass matrices, M_ν. For GR, $\alpha = (1+\sqrt{5})/2$ as given in the text.

Mixing	U	M_ν	A, B, C
TBM	$\begin{pmatrix} \frac{2}{\sqrt{6}} & \frac{1}{\sqrt{3}} & 0 \\ \frac{-1}{\sqrt{6}} & \frac{1}{\sqrt{3}} & \frac{-1}{\sqrt{2}} \\ \frac{-1}{\sqrt{6}} & \frac{1}{\sqrt{3}} & \frac{1}{\sqrt{2}} \end{pmatrix}$	$\begin{pmatrix} A & B & B \\ .. & \frac{1}{2}(A+B+C) & \frac{1}{2}(A+B-C) \\ .. & . & \frac{1}{2}(A+B+C) \end{pmatrix}$	$A = \frac{1}{3}(2m_1 + m_2 e^{-i\varphi_1})$, $B = \frac{1}{3}(m_2 e^{-i\varphi_1} - m_1)$, $C = m_3 e^{-i\varphi_2}$
BM	$\begin{pmatrix} \frac{1}{\sqrt{2}} & \frac{1}{\sqrt{2}} & 0 \\ \frac{-1}{2} & \frac{1}{2} & \frac{-1}{\sqrt{2}} \\ \frac{-1}{2} & \frac{1}{2} & \frac{1}{\sqrt{2}} \end{pmatrix}$	$\begin{pmatrix} A & B & B \\ .. & C & A-C \\ .. & . & C \end{pmatrix}$	$A = \frac{1}{2}(m_1 + m_2 e^{-i\varphi_1})$, $B = \frac{1}{2\sqrt{2}}(m_2 e^{-i\varphi_1} - m_1)$, $C = \frac{1}{4}(m_1 + m_2 e^{-i\varphi_1} + 2m_3 e^{-i\varphi_2})$
HM	$\begin{pmatrix} \frac{\sqrt{3}}{2} & \frac{1}{2} & 0 \\ \frac{-1}{2\sqrt{2}} & \frac{\sqrt{3}}{2\sqrt{2}} & \frac{-1}{\sqrt{2}} \\ \frac{-1}{2\sqrt{2}} & \frac{\sqrt{3}}{2\sqrt{2}} & \frac{1}{\sqrt{2}} \end{pmatrix}$	$\begin{pmatrix} A & B & B \\ .. & \frac{1}{2}(A+\sqrt{\frac{8}{3}}B+C) & \frac{1}{2}(A+\sqrt{\frac{8}{3}}B-C) \\ .. & . & \frac{1}{2}(A+\sqrt{\frac{8}{3}}B+C) \end{pmatrix}$	$A = \frac{1}{4}(3m_1 + m_2 e^{-i\varphi_1})$, $B = \frac{1}{4}\sqrt{\frac{3}{2}}(m_2 e^{-i\varphi_1} - m_1)$, $C = m_3 e^{-i\varphi_2}$
GR	$\begin{pmatrix} \frac{\alpha}{\sqrt{1+\alpha^2}} & \frac{1}{\sqrt{1+\alpha^2}} & 0 \\ \frac{-1}{\sqrt{2(1+\alpha^2)}} & \frac{\alpha}{\sqrt{2(1+\alpha^2)}} & \frac{-1}{\sqrt{2}} \\ \frac{-1}{\sqrt{2(1+\alpha^2)}} & \frac{\alpha}{\sqrt{2(1+\alpha^2)}} & \frac{1}{\sqrt{2}} \end{pmatrix}$	$\begin{pmatrix} A & B & B \\ .. & C & A+\sqrt{2}B-C \\ .. & . & C \end{pmatrix}$	$A = \frac{1}{(1+\alpha^2)}(m_1\alpha^2 + m_2 e^{-i\varphi_1})$, $B = \frac{1}{\sqrt{2}(1+\alpha^2)}(m_2 e^{-i\varphi_1} - m_1)\alpha$, $C = \frac{1}{2(1+\alpha^2)}(m_1 + m_2 e^{-i\varphi_1}\alpha^2) + \frac{1}{2}m_3 e^{-i\varphi_2}$

different in all four cases. Four different forms of mixing matrices and the corresponding light neutrino mass matrices considered here are shown in Table 2. All the above mixing scenarios can be presented by the matrix form written as

$$U = \begin{pmatrix} c_{12} & s_{12} & 0 \\ \frac{-s_{12}}{\sqrt{2}} & \frac{c_{12}}{\sqrt{2}} & \frac{-1}{\sqrt{2}} \\ \frac{-s_{12}}{\sqrt{2}} & \frac{c_{12}}{\sqrt{2}} & \frac{1}{\sqrt{2}} \end{pmatrix}, \tag{1.3}$$

where θ_{12} is given by $\arcsin(1/\sqrt{3})$ for TBM, $\pi/4$ for BM, $\pi/6$ for HM, and $\tan^{-1}(1/\alpha)$ with $\alpha = (1+\sqrt{5})/2$ for GR. Mixing angles in these scenarios are determined independent of the neutrino masses. The mass matrices having such diagonalizing mixing matrix are called mass independent textures or form diagonalizable textures [13]. There have been some studies earlier on the origin and effects of perturbations on these mixing scenarios [14] in order to accommodate non-zero θ_{13}.

Another attractive possibility is that those flavor symmetries are present at very high scale, namely, grand unified scale ($\Lambda_{GUT} \sim 10^{16}$ GeV). It has been found earlier in [15–17] that corrections from the renormalization group evolution (RGE) can significantly affect neutrino mixing angles, CP phases and mass splittings and thus, they should not be neglected in the models with flavor symmetries imposed at high energy scale.

In the framework of type I seesaw with three heavy right handed neutrinos [18], we study the radiative corrections to the masses and mixing angles of neutrinos in the charged lepton basis by the RGE [19–21] from $\Lambda_{\rm GUT}$ to $\Lambda_{\rm EW}$ ($\sim 10^2$ GeV), in addition to the seesaw threshold corrections [22–24]. Threshold corrections occur by subsequently integrating out heavy right handed Majorana masses at the respective seesaw scales both in the SM and MSSM. We assume that all the above mentioned specific mixing matrices are realized at GUT scale, and the corresponding

light neutrino mass matrices, M_ν, are given in terms of three masses as shown in Table 2. The heavy right handed neutrino mass matrices can be determined by inverting the seesaw formula. We first take the general form of the neutrino Dirac Yukawa matrix Y_ν and then pick its specific form that leads to the specific mixing pattern by scanning the parameter space. Below the seesaw threshold scales the RGE behavior is described by the effective theories which are governed by the effective mass operators. However, above all the seesaw threshold scales, we have to consider the full theory. The interplay of the heavy and the light sectors can modify the RGE effects, further on top of what were in the effective theory. In Ref. [23], the authors have studied RGE evolution of neutrino mixing angles and CP phases for some mixing scenarios at high scale by incorporating seesaw threshold effects and concluded that two of the considered mixing scenarios can lead to at most $\theta_{13} \sim 5^\circ$ at $\Lambda_{\rm EW}$. However, they do not fully consider the effects of the Majorana phases in the RGE evolution. Comparatively studying the RGE in absence and presence of Majorana phases, we find that these phases can give significant contributions in the running of neutrino flavor mixing angles. We have checked that turning off some CP phases in the present study reproduces the results almost similar to [23]. We have found that the measured reactor mixing angle, θ_{13}, up to 3σ C.L. can be achieved *only when* the Majorana phases are fully incorporated in the RGE from the GUT scale to electroweak scale. In fact, in order to realize such mixing scenarios, one may need to add additional Higgs bosons. The existence of the extra particles may affect the RG running, but those effects are highly model dependent. In particular, the RGEs for dimension five neutrino mass operator in the multi-Higgs doublet models are derived and their running has been performed in [25]. In this work, we assume that the contributions of extra particles to the RG running are negligibly small, which can be achieved by taking couplings to be small.

The paper is organized as follows. In Section 2, we discuss the specific forms of neutrino mass and mixing matrices for different mixing scenarios at the GUT scale. In Section 3, the RGE equations governing at various energy scales in addition to the seesaw threshold effects are presented. Section 4 gives the numerical results of our study both in the SM and the MSSM, respectively. We summarize our results in the last section.

2. Lepton mixing matrices at the GUT scale

In the basis where the charged lepton mass matrix is real and diagonal, the effective light neutrino mass matrix, M_ν, is in general given as

$$M_\nu = U^* P^* M_\nu^{diag} P^\dagger U^\dagger. \tag{2.1}$$

Here U has one of the forms given in Table 2. P is the phase matrix having two Majorana phases given as $\mathrm{Diag}(1, e^{-i\varphi_1/2}, e^{-i\varphi_2/2})$ and $M_\nu^{diag} = \mathrm{Diag}(m_1, m_2, m_3)$. The different form of the corresponding light neutrino mass matrices are given in Table 2. Following exactly the same procedure as given in Ref. [23], the Yukawa coupling matrix, Y_ν, is taken to be of the form

$$Y_\nu = y_\nu \cdot R \cdot Diag(r_1, r_2, 1). \tag{2.2}$$

The three real, positive and dimensionless parameters y_ν, r_1 and r_2 characterize the hierarchy of Y_ν and R is given as

$$R = R_{23}(\theta_2) \cdot R_{13}(\theta_3 e^{-i\delta}) \cdot R_{12}(\theta_1), \tag{2.3}$$

where R_{ij} are the rotation matrices in the ijth plane. The three mixing angles $(\theta_1, \theta_2, \theta_3)$ and a phase δ are free parameters varied randomly. Thus, Y_ν comprises of 7 free parameters, three

eigenvalues, three mixing angles and δ. The parameters y_ν, r_1 and r_2 are small $\leq \mathcal{O}(1)$. Thus, the effective RGEs between GUT scale and seesaw scales depend on Y_ν, Y_l and M_R. M_R can be determined by inverting seesaw formula given as

$$M_R = -Y_\nu M_\nu^{-1} Y_\nu^T. \tag{2.4}$$

Transferring to the basis where M_R is diagonal,

$$U_R^T M_R U_R = Diag(M_{R_1}, M_{R_2}, M_{R_3}). \tag{2.5}$$

Y_ν gets simultaneously transformed as $Y_\nu U_R^*$. Since M_R in our analysis is hierarchical i.e. $M_{R_1} < M_{R_2} < M_{R_3}$ we consider the seesaw threshold effects which arise due to sequential decoupling of these fields at respective scales. For the normal hierarchical spectrum the lowest neutrino mass, m_1 is a free parameter. The other two masses m_2 and m_3 are determined by the relation $m_2 = \sqrt{m_1^2 + \Delta m_{12}^2}$ and $m_3 = \sqrt{m_1^2 + \Delta m_{13}^2}$ where Δm_{12}^2 and Δm_{13}^2 are the solar and the atmospheric mass squared differences, respectively. We present the numerical analysis for normal hierarchical spectrum where m_1 is the smallest mass. Since the running of the mixing angles is inversely proportional to masses there can be more corrections to those angles for the quasidegenerate and inverted mass spectrum in these mixing scenarios [21]. Yet, we focus on whether the measurements on θ_{13} can be achieved by RG running in the normal hierarchical spectrum, within the most conservative scenario.

3. RGE equations in the presence of seesaw threshold effects

Extended by three right handed neutrinos, the leptonic Yukawa terms of the Lagrangian in the SM can be written as

$$-\mathcal{L}_{(\mathrm{SM})} = \bar{l}_l H Y_l l_R + \bar{l}_l \tilde{H} Y_\nu \nu_R + \frac{1}{2} \bar{\nu^c}_R M_R \nu_R + \mathrm{h.c.} \tag{3.1}$$

For the MSSM it is

$$-\mathcal{L}_{(\mathrm{MSSM})} = \bar{l}_l H_1 Y_l l_R + \bar{l}_l \tilde{H}_2 Y_\nu \nu_R + \frac{1}{2} \bar{\nu^c}_R M_R \nu_R + \mathrm{h.c.}, \tag{3.2}$$

where H ($\tilde{H} = i\sigma^2 H^*$) is the SM Higgs doublet (H_1, H_2 for MSSM), l_l, e_R, ν_R are the lepton $SU(2)_L$ doublet, right handed charged leptons and right handed neutrinos, respectively. The current neutrino mixing angles and mass squared differences are determined from the neutrino oscillation experiments at the low energy scale. The seesaw threshold corrections can be quite significant at the seesaw scales as the heavy singlets can be nondegenerate i.e. $M_{R_1} < M_{R_2} < M_{R_3}$. In the flavor basis the effective light neutrino mass matrix, M_ν, above the highest seesaw scale is given to be

$$M_\nu(\mu) = -\frac{\kappa(\mu) v^2}{4}, \tag{3.3}$$

here $v = 246$ GeV in the SM and $(246\ \mathrm{GeV}) \cdot \sin\beta$ in the MSSM, μ is the renormalization scale and κ is the effective coupling matrix given as

$$\kappa(\mu) = 2 Y_\nu^T(\mu) M_R^{-1}(\mu) Y_\nu(\mu). \tag{3.4}$$

For the running of neutrino parameters above the seesaw scales we use the formulae given in [22]. The radiative corrections from the GUT to M_{R_3} comprises of running of the Yukawa couplings

Y_ν, M_R and Y_l. We work in the basis where charged lepton is diagonal. In the course of running there are additional contributions generated from off-diagonal entries of $Y_l^\dagger Y_l$, which are taken into consideration while calculating the total mixing matrix as $U_l^\dagger U_\nu$. The effective operator at the heaviest scale, M_{R_3} is given by the matching condition

$$\kappa^{(3)} = 2Y_\nu^T M_{R_3}^{-1} Y_\nu, \tag{3.5}$$

in the basis where M_R is diagonal. The effective neutrino mass matrix at the scale below M_{R_3} now constitutes of two parts

$$M_\nu = -\frac{v^2}{4}[\kappa^{(3)} + 2Y_\nu^{T(3)} M_R^{-1(3)} Y_\nu^{(3)}], \tag{3.6}$$

where $Y_\nu^{(3)}$ is 2×3 and $M_R^{(3)}$ is the 2×2 mass matrix remained after decoupling M_{R_3}. Following the same procedure at $\mu = M_{R_2}$ the Yukawa coupling matrix is further reduced to 1×3 matrix. The one loop RGE for $\kappa^{(1)}$ after decoupling all the three heavy right handed fields [22] is given as

$$16\pi^2 \frac{d\kappa^{(1)}}{dt} = (C_\nu^l (Y_l^\dagger Y_l)^T)\kappa^{(1)} + \kappa^{(1)}(C_\nu^l (Y_l^\dagger Y_l)) + \alpha\kappa^{(1)}, \tag{3.7}$$

where parameter α is explicitly given by

$$\begin{aligned} \alpha_{\rm SM} &= 2\ Tr(3Y_u^\dagger Y_u + 3Y_d^\dagger Y_d + Y_l^\dagger Y_l) - 3g_2^2 + \lambda, \\ \alpha_{\rm MSSM} &= 2\ Tr(3Y_u^\dagger Y_u) - \frac{6}{5}g_1^2 - 6g_2^2. \end{aligned} \tag{3.8}$$

The effective neutrino mass matrix obtained from $\kappa^{(1)}$ at the EW scale is diagonalized to obtain the neutrino mixing angles, CP violating phases and mass squared differences.

The neutrino mass matrices at two different scales Λ_{GUT} and Λ_{EW} are homogeneously related as [26,27]

$$M_\nu^{\Lambda_{EW}} = I_K I_\kappa^T M_\nu^{\Lambda_{GUT}} I_\kappa, \tag{3.9}$$

here I_K is the scale factor common to all elements of $M_\nu^{\Lambda_{EW}}$. The matrix I_κ is given as

$$I_\kappa = Diag(\sqrt{I_e}, \sqrt{I_\mu}, \sqrt{I_\tau}). \tag{3.10}$$

In the presence of seesaw threshold corrections [28] we have

$$\sqrt{I_j} = Exp(-\frac{1}{16\pi^2}\int [3(Y_j^\dagger Y_j) - (Y_{\nu_j}^\dagger Y_{\nu_j})]dt) = e^{-\Delta_j},$$

j $= e$, μ and τ. From this relation when $Y_\tau \sim 0.01$ and $Y_{\nu_\tau} \sim 0.3$, the magnitude of Δ_τ can be of the order of 10^{-3} in the SM ($10^{-3}(1+\tan^2\beta)$ in the MSSM) from 10^{12} GeV to 10^2 GeV. It is worthwhile to notice that in presence of threshold effects, the magnitudes of Δ_e and Δ_μ can be comparable to Δ_τ for large values of Y_{ν_e} and Y_{ν_μ}. Thus, Δ_e and Δ_μ terms in the presence of threshold effects can play an important role in enhancing RGE corrections. In the absence of threshold effects when Y_{ν_τ} is absent, Δ_τ is of the order of 10^{-5} and Δ_e, Δ_μ contributions are very small and thus can be neglected.

Below the seesaw scales where all the heavy right handed fields are integrated out, the running in the SM is mostly governed by $Y_\tau \sim \sqrt{2}m_\tau/v \approx \mathcal{O}(10^{-2})$ and $Y_\tau \sim \sqrt{2}m_\tau/(v\cos\beta)$ in

the MSSM. There are no significant corrections to mixing angles in the SM even for quasidegenerate spectrum of masses in this region. In the MSSM case, however, there can be significant corrections when $\tan\beta$ is large. The analytic expressions of the RGE of masses, mixing angles and CP phases below the seesaw scales are given in [21] and the expressions for running above the seesaw scales are given in [22,24] in detail.

4. Numerical results

We begin at $\Lambda_{\rm GUT}$ by varying the three angles and phase of Y_ν along with two Majorana phases in the range of 0–2π. Three hierarchical parameters of Y_ν and m_1 are also randomly varied. We note that the Dirac phase δ_{CP} is not well defined when θ_{13} becomes zero at the GUT scale. In Ref. [21] the analytical continuation condition is derived that assures $\frac{d\delta_{CP}}{dt}$ is finite and running of δ_{CP} is extended continuously even when θ_{13} approaches to zero. Following [21], we can avoid the divergence happened in the running of δ_{CP}. Since there are lots of free parameters, it is hard to obtain full parameter space in consistent with experimental data up to 3σ C.L. Instead, we present some sets of input parameter space which lead to maximally allowed value of θ_{13} achieved at low scale, while the other mixing angles and mass squared differences are simultaneously in the ranges of measured values up to 3σ.

4.1. RGE and seesaw threshold corrections in the SM

In this analysis we start with different neutrino mass matrices, M_ν, that are diagonalized by the mixing matrices, U given in Table 2, respectively. Running of the RGE can be divided into three regions governed by different RG equations in the respective regions as

a) from $\Lambda_{\rm GUT}$ down to the highest seesaw scale M_{R_3},
b) in between the three seesaw scales,
c) from the lowest seesaw scale M_{R_1} down to $\Lambda_{\rm EW}$.

At the leading order the expression for θ_{12} is inversely proportional to solar mass squared difference (Δm^2_{12}), whereas the other mixing angles θ_{23} and θ_{13} are both inversely related to atmospheric mass squared difference (Δm^2_{13}). Thus, θ_{12} is maximally affected by the RGE among all the mixing angles. In case of quasidegenerate neutrino spectrum there can be visible corrections to other mixing angles also. In the SM, RGE corrections to neutrino mixing angles in absence of threshold corrections are negligible. However, inclusion of the threshold effects can significantly modify RGE of neutrino masses. We study the RGE of neutrino mixing angles from $\Lambda_{\rm GUT}$ to $\Lambda_{\rm EW}$ in the SM for zero and non-zero Majorana phases in all four mixing scenarios.

The behaviors of RGE for mixing angles θ_{12}, θ_{23} and θ_{13} in all cases are shown in Figs. 1, 2, 3 and 4 for TBM, BM, HM and GR, respectively. In those figures, the left panel corresponds to $\varphi_1 = \varphi_2 = 0$, while the right panel has non-zero φ_1 and φ_2. The set of input parameters taken at $\Lambda_{\rm GUT}$ corresponding to each cases are given in the second and third columns of Tables 3, 4, 5 and 6, respectively. The last two columns in those tables correspond to the output parameters obtained at $\Lambda_{\rm EW}$. The effects of RGEs for the neutrino mixing angles below the lowest seesaw scale M_{R_1} down to $\Lambda_{\rm EW}$ are negligible in the SM because of small corrections arisen only due to Y_l.

However, at the energy scale between and above the seesaw scales, there will be additional contributions of Y_ν along with Y_l. Thus, the RGE is dependent on Y_ν which is free and can be

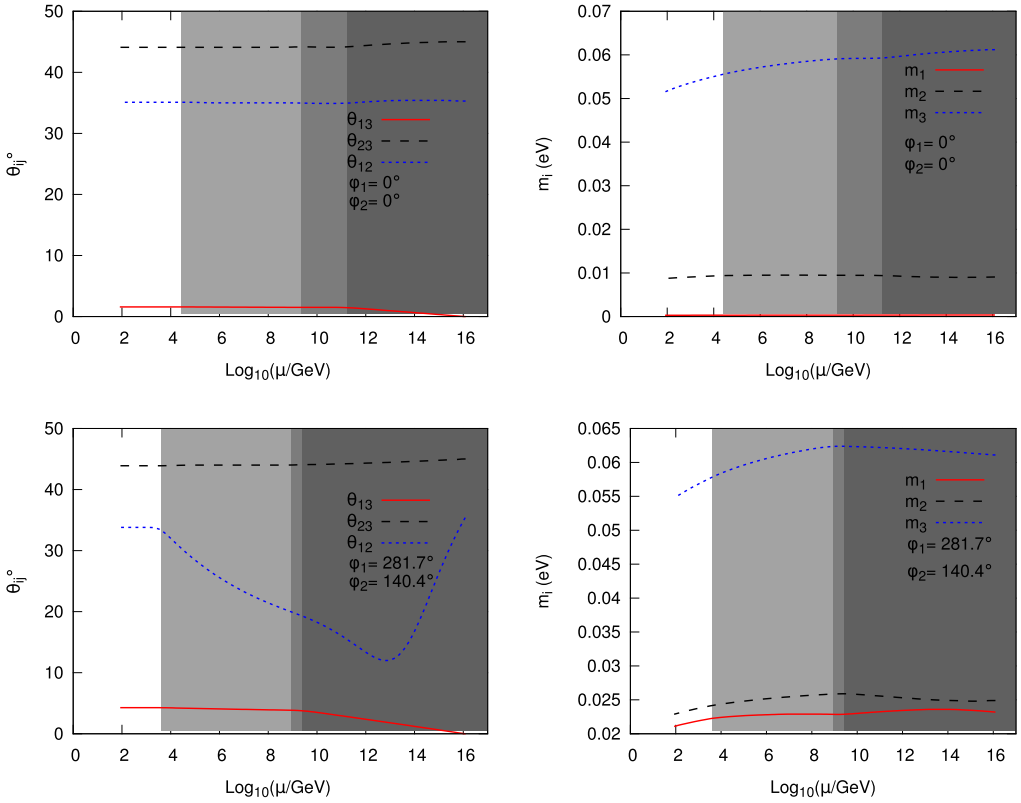

Fig. 1. The RGE of mixing angles and masses in the SM for TBM mixing. The input parameters are given in the second and third column of Table 3. The grey shaded areas illustrate the ranges of effective theories when heavy right handed singlets are integrated out.

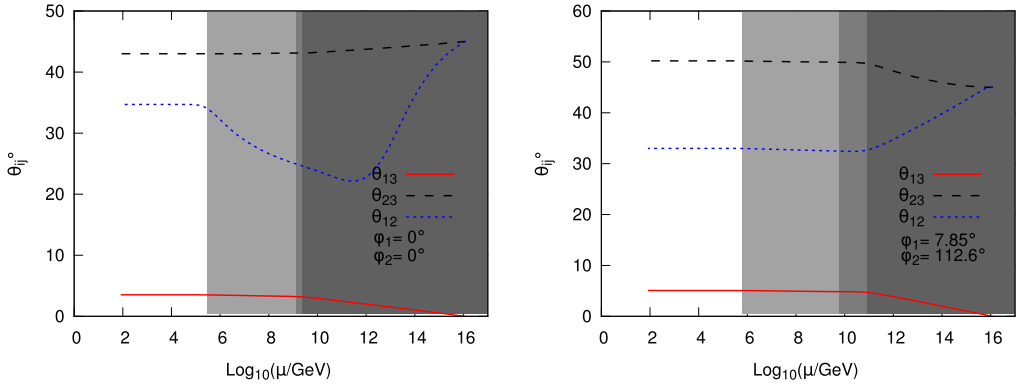

Fig. 2. The RGE of mixing angles in the SM for BM mixing. The input parameters are given in the second and third column of Table 4. The grey shaded areas illustrate the ranges of effective theories when heavy right handed singlets are integrated out.

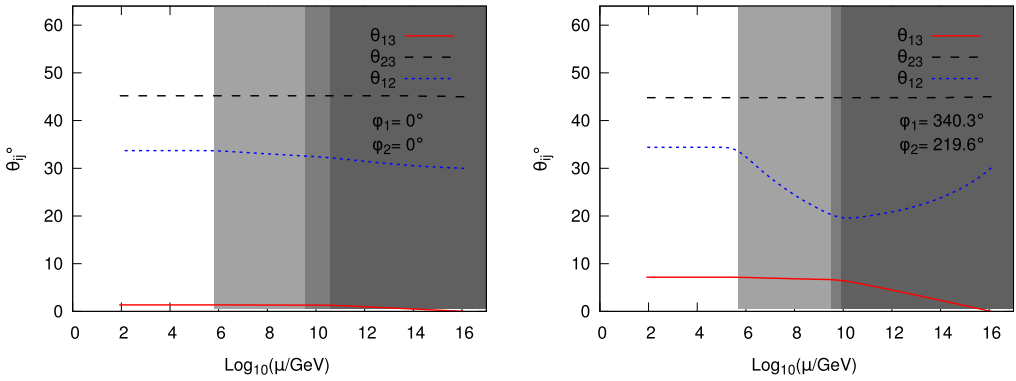

Fig. 3. The RGE of mixing angles in the SM for HM mixing. The input parameters are given in the second and third column of Table 5. The grey shaded areas illustrate the ranges of effective theories when heavy right handed singlets are integrated out.

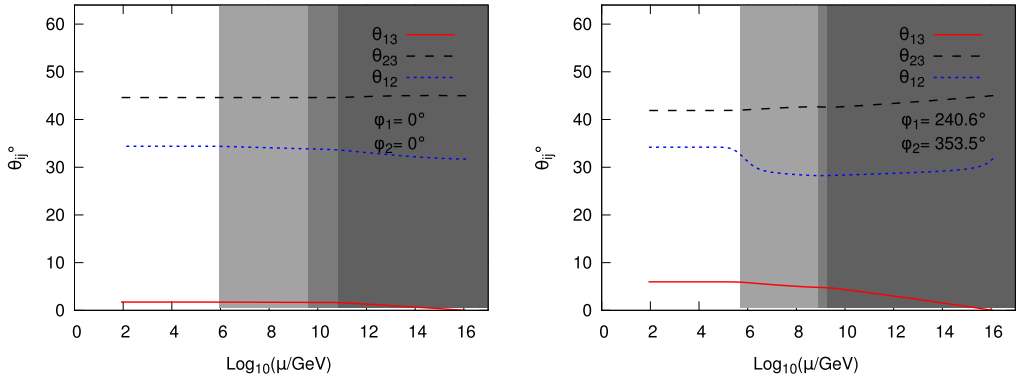

Fig. 4. The RGE of mixing angles in the SM for GR mixing. The input parameters are given in the second and third column of Table 6. The grey shaded areas illustrate the ranges of effective theories when heavy right handed singlets are integrated out.

as large as $\mathcal{O}(1)$. Heavy right handed fields are subsequently integrated out at the three seesaw scales shown by the three grey regions in the figures. Thus $(n-1)\times 3$ submatrix of Y_ν remains after each step of integrating out M_{R_i}. As can be seen from Eq. (3.6), the running between the seesaw scales is dependent on the sum of two terms $\kappa^{(n)}$ and $2Y_\nu^{T(n)}M_R^{(n)}Y_\nu^{(n)}$. As discussed in [22], in the SM the RGE scaling in these two terms is different due to interaction with trivial flavor structure. This implies that there can be large corrections for the mixing angles between these threshold scales in the SM. The values of three seesaw scales are given in the output column of Tables 3, 4, 5 and 6. From Eq. (2.4), the heavy right handed Majorana masses in the TBM at the GUT scale for vanishing Majorana phases are found to be $M_{R_i} = 2.62\times 10^4$ eV, 2.23×10^9 eV, 1.75×10^{11} eV respectively. We observe small running of these values between GUT and seesaw scales. There are significant corrections to mixing angles especially θ_{12} between and above the seesaw scales for non-zero Majorana phases in the SM, whereas small running for vanishing φ_1 and φ_2 as shown in Figs. 1, 2, 3 and 4. We found that small value of $\theta_{13} < 3.5°$ is obtained for vanishing Majorana phases. However, when these phases are non-zero θ_{13} as large as 6.9° is

Table 3
Numerical values of input and output parameters radiatively generated in the SM for TBM mixing for zero and non-zero Majorana phases at $\Lambda_{GUT} = 2 \times 10^{16}$ GeV. The input values for neutrino mixing angles at the GUT scale are $\theta_{13} = 0°$, $\theta_{23} = 45°$ and $\theta_{12} = 35.3°$.

SM input	$\varphi_1, \varphi_2 = 0$	$\varphi_1, \varphi_2 \neq 0$	SM output	$\varphi_1, \varphi_2 = 0$	$\varphi_1, \varphi_2 \neq 0$
r_1	0.57×10^{-3}	0.83×10^{-3}	M_{R_1} (GeV)	2.6×10^{4}	4×10^{3}
r_2	0.6	0.47	M_{R_2} (GeV)	2.1×10^{9}	8.2×10^{8}
δ	14.7°	28.36°	M_{R_3} (GeV)	1.7×10^{11}	2.5×10^{9}
y_ν	0.5	0.35	–	–	–
θ_1	216°	194.2°	θ_{12}	35.1°	33.8°
θ_2	168°	81.36°	θ_{23}	44.1°	43.9°
θ_3	80.8°	350.6°	θ_{13}	1.6°	4.3°
m_1 (eV)	3.6×10^{-4}	0.023	m_1 (eV)	2.94×10^{-4}	0.021
Δm^2_{12} (eV^2)	8.2×10^{-5}	8.0×10^{-5}	Δm^2_{12} (eV^2)	7.63×10^{-5}	7.86×10^{-5}
Δm^2_{13} (eV^2)	3.7×10^{-3}	3.3×10^{-3}	Δm^2_{13} (eV^2)	2.6×10^{-3}	2.48×10^{-3}
φ_1	0°	281.7°	φ_1	124°	351°
φ_2	0°	140.4°	φ_2	138°	227.5°
–	–	–	J_{CP}	5.8×10^{-3}	0.016
–	–	–	M_{ee} (eV)	2.85×10^{-3}	0.02

Table 4
Numerical values of input and output parameters radiatively generated in the SM for BM mixing for zero and non-zero Majorana phases at $\Lambda_{GUT} = 2 \times 10^{16}$ GeV. The input values for neutrino mixing angles at GUT scale are $\theta_{13} = 0°$, $\theta_{23} = \theta_{12} = 45°$.

SM input	$\varphi_1, \varphi_2 = 0$	$\varphi_1, \varphi_2 \neq 0$	SM output	$\varphi_1, \varphi_2 = 0$	$\varphi_1, \varphi_2 \neq 0$
r_1	0.64×10^{-2}	0.24×10^{-2}	M_{R_1} (GeV)	3×10^{5}	6.5×10^{5}
r_2	0.65	0.703	M_{R_2} (GeV)	1.27×10^{9}	5.8×10^{9}
δ	243°	268°	M_{R_3} (GeV)	2.4×10^{9}	8×10^{10}
y_ν	0.37	0.74	–	–	–
θ_1	243°	163°	θ_{12}	34.7°	33°
θ_2	60.2°	329°	θ_{23}	43°	50.2°
θ_3	306°	333.5°	θ_{13}	3.52°	5.07°
m_1 (eV)	0.0264	4.8×10^{-3}	m_1 (eV)	0.0243	1.58×10^{-3}
Δm^2_{12} (eV^2)	1.5×10^{-4}	4.8×10^{-7}	Δm^2_{12} (eV^2)	7.03×10^{-5}	7.94×10^{-5}
Δm^2_{13} (eV^2)	3.07×10^{-3}	3.4×10^{-3}	Δm^2_{13} (eV^2)	2.4×10^{-3}	2.36×10^{-3}
φ_1	0°	7.85°	φ_1	4°	2.8°
φ_2	0°	112.6°	φ_2	3.05°	90°
–	–	–	J_{CP}	-7.3×10^{-4}	−0.01
–	–	–	M_{ee} (eV)	4.14×10^{-3}	0.024

produced. In all four cases, there is considerable corrections to θ_{12} and it is possible to obtain it's value near the best fit (33°) at the low scale when it ranges from (30°–45°) at the high GUT scale. In the absence of the Majorana phases it is not possible to have large values of θ_{13} at the low scale in the SM. In Ref. [23] it has been shown that in the SM θ_{13} as large as 5° can only be obtained when very large $\theta_{12} = 67°$ is considered at the GUT scale. However, taking into consideration the Majorana phases, θ_{13} as large as $\approx 5°$– 6.9° is obtained at the low scale when θ_{12} at Λ_{GUT} is in the range of (30°–45°). Thus, the Majorana phases can significantly affect the RGE of neutrino mixing angles [29] as observed above. However, in the SM, the value of θ_{13} is still below 3σ allowed range at low scale for both zero and non-zero Majorana phases.

Table 5
Numerical values of input and output parameters radiatively generated in the SM for HM mixing for zero and non-zero Majorana phases at $\Lambda_{GUT} = 2 \times 10^{16}$ GeV. The input values for neutrino mixing angles at GUT scale are $\theta_{13} = 0°$, $\theta_{23} = 45°$ and $\theta_{12} = 30°$.

SM input	$\varphi_1, \varphi_2 = 0$	$\varphi_1, \varphi_2 \neq 0$	SM output	$\varphi_1, \varphi_2 = 0$	$\varphi_1, \varphi_2 \neq 0$
r_1	0.29×10^{-2}	0.63×10^{-2}	M_{R_1} (GeV)	6.4×10^5	4.7×10^5
r_2	0.57	0.68	M_{R_2} (GeV)	3.3×10^9	3.1×10^9
δ	23.1°	337.5°	M_{R_3} (GeV)	3.7×10^{10}	7.6×10^9
y_ν	0.661	0.59	–	–	–
θ_1	146°	147.2°	θ_{12}	33.7°	34.4°
θ_2	261°	271.6°	θ_{23}	45.2°	44.8°
θ_3	175.3°	92.25°	θ_{13}	1.4°	6.9°
m_1 (eV)	4.14×10^{-3}	0.0294	m_1 (eV)	3.38×10^{-3}	0.0245
Δm^2_{12} (eV^2)	9.6×10^{-5}	8.6×10^{-5}	Δm^2_{12} (eV^2)	7.4×10^{-5}	7.63×10^{-5}
Δm^2_{13} (eV^2)	3.65×10^{-3}	3.8×10^{-3}	Δm^2_{13} (eV^2)	2.4×10^{-3}	2.6×10^{-3}
φ_1	0°	340.3°	φ_1	160.2°	25.9°
φ_2	0°	219.6°	φ_2	151.4°	242°
–	–	–	J_{CP}	-5.36×10^{-3}	−0.024
–	–	–	M_{ee} (eV)	4.9×10^{-3}	0.022

Table 6
Numerical values of input and output parameters radiatively generated in the SM for GR mixing for zero and non-zero Majorana phases at $\Lambda_{GUT} = 2 \times 10^{16}$ GeV. The input neutrino mixing angles at GUT scale are $\theta_{13} = 0°$, $\theta_{23} = 45°$ and $\theta_{12} = 31.7°$.

SM input	$\varphi_1, \varphi_2 = 0$	$\varphi_1, \varphi_2 \neq 0$	SM output	$\varphi_1, \varphi_2 = 0$	$\varphi_1, \varphi_2 \neq 0$
r_1	0.27×10^{-2}	0.68×10^{-3}	M_{R_1} (GeV)	8.7×10^5	4.9×10^5
r_2	0.6	0.35	M_{R_2} (GeV)	4×10^9	7.7×10^8
δ	55.2°	63.0°	M_{R_3} (GeV)	6.6×10^{10}	1.8×10^9
y_ν	0.7	0.65	–	–	–
θ_1	46.8°	192.5°	θ_{12}	34.4°	34.2°
θ_2	225°	185.6°	θ_{23}	44.6°	41.9°
θ_3	123°	249°	θ_{13}	1.73°	6°
m_1 (eV)	2.1×10^{-3}	0.079	m_1 (eV)	1.62×10^{-3}	0.067
Δm^2_{12} (eV^2)	8.9×10^{-5}	9.3×10^{-5}	Δm^2_{12} (eV^2)	7.25×10^{-5}	7.6×10^{-5}
Δm^2_{13} (eV^2)	3.7×10^{-3}	3.8×10^{-3}	Δm^2_{13} (eV^2)	2.3×10^{-3}	2.3×10^{-3}
φ_1	0°	240.6°	φ_1	171°	13.6°
φ_2	0°	353.5°	φ_2	185°	107.5°
–	–	–	J_{CP}	0.007	−0.02
–	–	–	M_{ee} (eV)	3.8×10^{-3}	0.06

In Fig. 1 we also show the RGE of the neutrino masses from Λ_{GUT} to Λ_{EW} for both zero and non-zero Majorana phases in the TBM. The running of the mass eigenvalues in this region below the seesaw scales can be significant in the SM due to the factor α Eq. (3.8) which can be larger than Y_τ^2. As we see from the right panel of Fig. 1 there is running of masses even below M_{R_1}, irrespective of values of φ_1 and φ_2. It indicates running of masses is not directly dependent on the Majorana phases [30]. Due to radiative generation of non-zero values of θ_{13} and δ_{CP} below the GUT scale, non-vanishing values of Jarlskog rephasing invariant are generated at Λ_{EW}, which lead to observable CP violation in neutrino oscillation experiments. For the best fit values of mixing angles and Dirac phase δ_{CP} (300°) given in the global analysis [7], the Jarlskog Invariant

is determined to be $J_{CP} = -0.028$. In the SM for non-vanishing Majorana phases we obtain $J_{CP} \sim -10^{-2}$ at the EW scale for BM, HM and GR scenarios. The measurement of δ_{CP} from long baseline neutrino oscillation experiments in future would be useful to study the viability of these mixing scenarios at high scale.

Neutrinoless double beta decay ($0\nu\beta\beta$) if observed, would imply lepton number violation (LNV) and Majorana nature of neutrinos. The current experimental results for $0\nu\beta\beta$ can constrain the effective Majorana neutrino mass, M_{ee}. From the search for $0\nu\beta\beta$ of ^{136}Xe at EXO-200 [31], the effective Majorana mass M_{ee} is constrained to be less than (0.14–0.38) eV at 90% C.L. A combination of limits from KamLAND-Zen [32] and EXO-200 constrains this limit further to less than (0.12–0.25) eV at 90% C.L. based on representative range of available matrix element calculations. The predictions of M_{ee} for all for four mixing scenarios are given in corresponding tables. Here $M_{ee} \sim 10^{-3}$ eV is obtained for vanishing phases while $\sim 10^{-2}$ eV is obtained when Majorana phases contribute to the RGE. The observations of the signal in the present and future $0\nu\beta\beta$ experiments will be crucial to decide the fate of these scenarios under consideration.

4.2. RGE and seesaw threshold corrections in the MSSM

The study of radiative corrections in the MSSM in presence of seesaw threshold effects can again be divided into three regions as in the SM. All these regions will be governed by different RGE equations, respectively. The RGE corrections to the mixing angles in the MSSM for region below seesaw scales can be larger than the SM due to the presence of factor $Y_\tau^2\ (1 + \tan^2\beta)$. This term can be large when $\tan\beta$ is large, thus, resulting in significant changes in the mixing angles where Y_l is the only contributing term. We study the RGE of mixing angles with zero and non-zero Majorana phases in the MSSM with $\tan\beta = 10$.

As seen in Figs. 5, 6, 7 and 8, the RGE running effects are small below lowest seesaw scale M_{R_1} down to the EW scale for $\tan\beta = 10$. In the region above seesaw scale, M_{R_3} there is large running of all the mixing angles as can be seen from the figures of all mixing scenarios in the MSSM. This is due to the contribution of Y_ν which can be large regardless to value of $\tan\beta$ in addition of Y_l. We have the large running of all mixing angles including θ_{13} in this region when Majorana phases are non-zero. Between the seesaw scale there is very small running in comparison to the SM. This behavior is described in Ref. [22] in detail as the enhanced running between the threshold scales due to the term with trivial flavor structure is absent in the MSSM. For vanishing Majorana phases, $\theta_{13} < 3.7^\circ$ is obtained in all mixing scenarios. However, when Majorana phases are considered the largest possible value of $\theta_{13} \approx 9.46^\circ$ is obtained in the TBM mixing. We get θ_{13} within its allowed 3σ range at the low scale in all scenarios. The Majorana phases play an important role in the enhancement of RGE and thus, θ_{13} can be produced in its 3σ allowed range at the EW scale in all mixing scenarios along with the other neutrino oscillation parameters. Three seesaw scales M_{R_i}, given in output of all tables are determined from Eqs. (2.4), (2.5). For the MSSM, in TBM when Majorana phases are zero we get M_{R_i} as 9.85×10^3 eV, 2.2×10^9 eV, 4.3×10^{10} eV at the GUT scale using Eq. (2.4). The different seesaw threshold scales in this case are given in Table 7. There is small difference in the values due to running between the GUT and seesaw scales. Running of M_{r_1} towards higher value is observed here.

We also see the radiative corrections to the masses in Fig. 5. The running of masses, however, as in the SM is independent of the mixing parameters since α is usually much larger than Y_τ^2 $(1 + \tan^2\beta)$ except in the MSSM with large $\tan\beta$. RGE effects of neutrino masses are smallest if $\tan\beta = 10$. The negligible running of masses is seen below the seesaw scales irrespective of values of φ_1 and φ_2 which indicate that the running of masses is not directly dependent on the

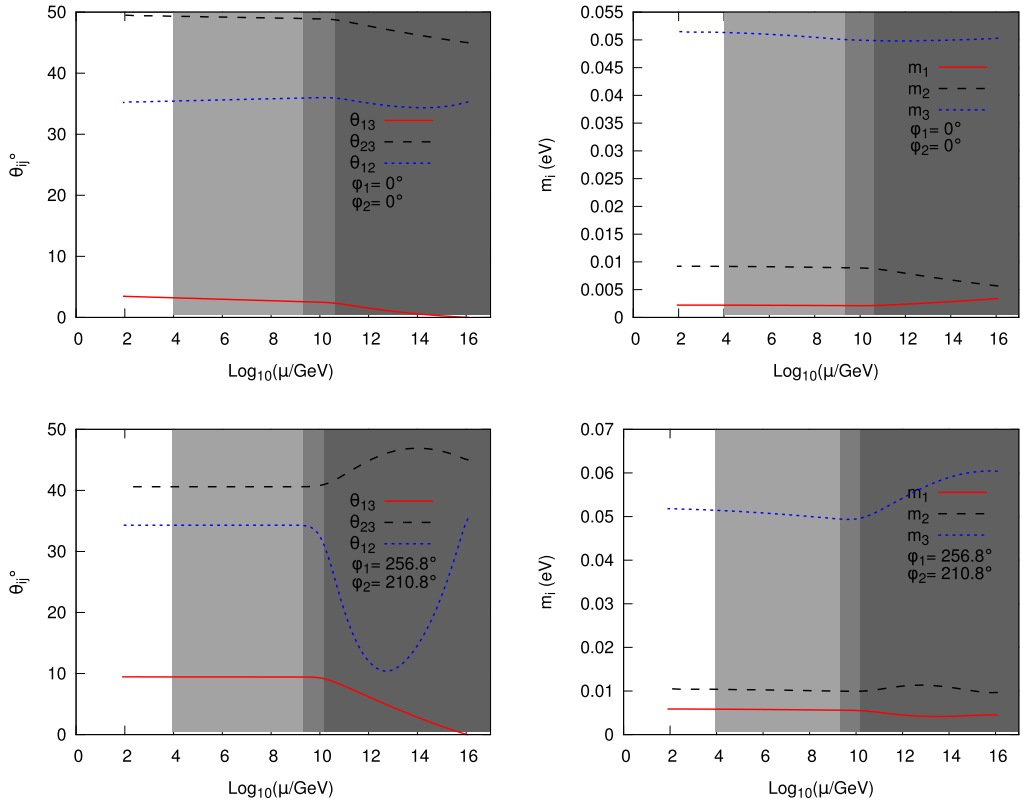

Fig. 5. The RGE of the mixing angles and masses in the MSSM with $\tan\beta = 10$. The input parameters are given in the second and third column of Table 7. The grey shaded areas illustrate the ranges of effective theories when heavy right handed singlets are integrated out.

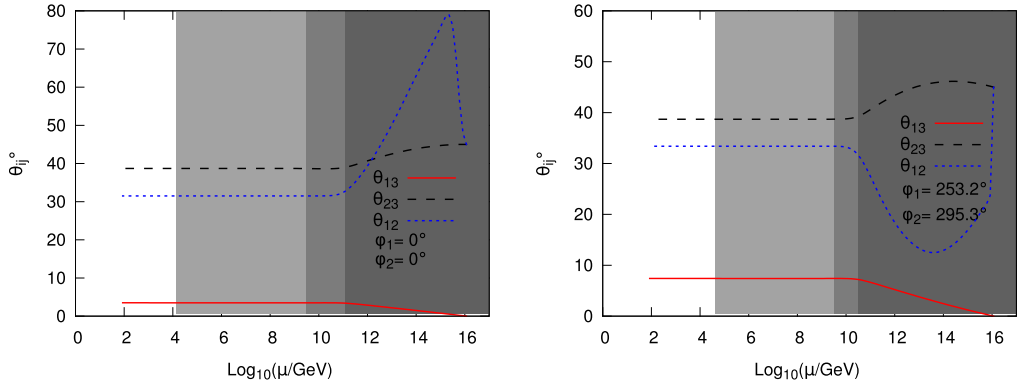

Fig. 6. The RGE of the mixing angles between $\Lambda_{\rm GUT}$ and $\Lambda_{\rm EW}$ in the MSSM with $\tan\beta = 10$ for BM mixing. The input parameters are given in second and third column of Table 8. The grey shaded areas illustrate the ranges of effective theories when heavy right handed singlets are integrated out.

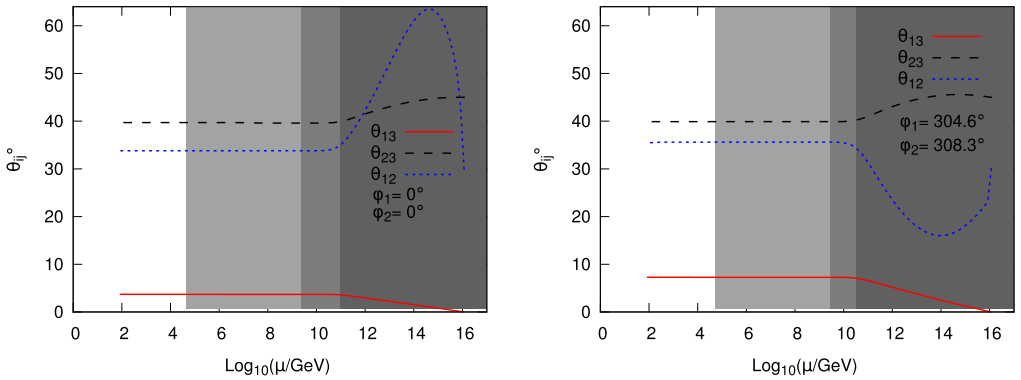

Fig. 7. The RGE of the mixing angles between Λ_{GUT} and Λ_{EW} in the MSSM with $\tan\beta = 10$ for HM mixing. The input parameters are given in the second and third column of Table 9. The grey shaded areas illustrate the ranges of effective theories when heavy right handed singlets are integrated out.

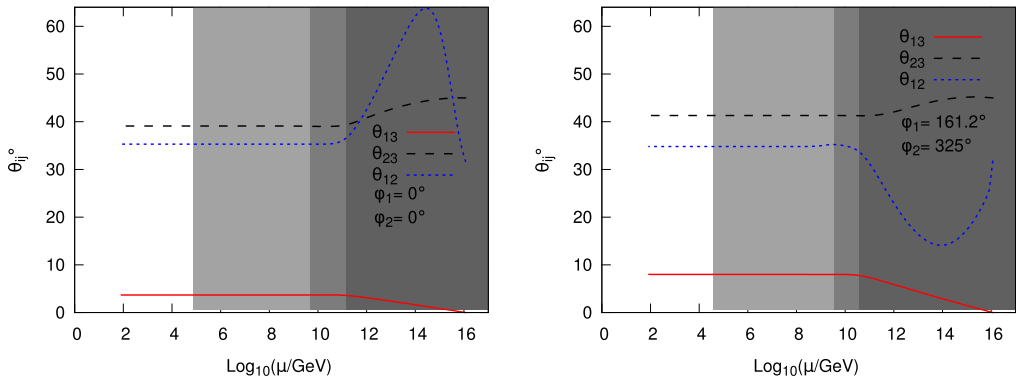

Fig. 8. The RGE of the mixing angles between Λ_{GUT} and Λ_{EW} in the MSSM with $\tan\beta = 10$ for GR mixing. The initial values of the parameters are given in the third column of Table 10. The grey shaded areas illustrate the ranges of effective theories when heavy right handed singlets are integrated out.

Majorana phases [30]. From RGEs of mixing angles and the Dirac phase δ_{CP} which depend on the Majorana phases, we obtain $J_{CP} \approx 10^{-2}$ and the effective Majorana mass $M_{ee} \approx 10^{-3}$ eV at low scale for all mixing scenarios. Thus, large value of θ_{13} which is in its present 3σ range at EW scale can be produced in the MSSM for $\tan\beta = 10$ when φ_1 and φ_2 are both non-zero at high scale.

5. Conclusions

We assume different lepton mixing matrices at the high energy (GUT) scale and study effects of the RGE and seesaw threshold corrections to these mixing scenarios both in the SM and MSSM. In the absence of seesaw threshold effects there are very small corrections both in the SM and MSSM. Significant corrections are observed both in the SM and MSSM when threshold effects are included. Above the seesaw scales there are more number of parameters due to Y_ν that can significantly affect the RGE of mixing angles. Below the lowest seesaw scale, contribution of Y_ν is absent and the RGE corrections are only due to Y_l which is very small in the SM and MSSM

Table 7
Numerical values of input and output parameters radiatively generated in the MSSM for TBM mixing for zero and non-zero Majorana phases at $\Lambda_{\rm GUT} = 2 \times 10^{16}$ GeV and $\tan\beta = 10$. The input values for neutrino mixing angles at GUT scale are $\theta_{13} = 0°$, $\theta_{23} = 45°$ and $\theta_{12} = 35.3°$.

MSSM input	$\varphi_1, \varphi_2 = 0$	$\varphi_1, \varphi_2 \neq 0$	MSSM output	$\varphi_1, \varphi_2 = 0$	$\varphi_1, \varphi_2 \neq 0$
r_1	0.36×10^{-3}	0.42×10^{-3}	M_{R_1} (GeV)	9.9×10^{3}	9.13×10^{3}
r_2	0.47	0.68	M_{R_2} (GeV)	2.1×10^{9}	2.04×10^{9}
δ	238°	196°	M_{R_3} (GeV)	4.0×10^{10}	1.36×10^{10}
y_ν	0.56	0.46	–	–	–
θ_1	176°	300.2°	θ_{12}	35.2°	34.3°
θ_2	256°	13.06°	θ_{23}	49.5°	40.6°
θ_3	66.5°	124.9°	θ_{13}	3.46°	9.46°
m_1 (eV)	3.4×10^{-3}	4.5×10^{-3}	m_1 (eV)	2.2×10^{-3}	5.9×10^{-3}
Δm^2_{12} (eV^2)	2.1×10^{-5}	7.33×10^{-5}	Δm^2_{12} (eV^2)	8×10^{-5}	7.48×10^{-5}
Δm^2_{13} (eV^2)	2.5×10^{-3}	3.56×10^{-3}	Δm^2_{13} (eV^2)	2.56×10^{-3}	2.57×10^{-3}
φ_1	0°	256.8°	φ_1	50.0°	112.7°
φ_2	0°	210.8°	φ_2	30°	10.5°
–	–	–	J_{CP}	-3.6×10^{-3}	−0.0156
–	–	–	M_{ee} (eV)	3.3×10^{-3}	3.7×10^{-3}

Table 8
Numerical values of input and output parameters radiatively generated in the MSSM for BM mixing for zero and non-zero Majorana phases at $\Lambda_{GUT} = 2 \times 10^{16}$ GeV and $\tan\beta = 10$. The input values for neutrino mixing angles at GUT scale are $\theta_{13} = 0°$, $\theta_{23} = \theta_{12} = 45°$.

MSSM input	$\varphi_1, \varphi_2 = 0$	$\varphi_1, \varphi_2 \neq 0$	MSSM output	$\varphi_1, \varphi_2 = 0$	$\varphi_1, \varphi_2 \neq 0$
r_1	0.274×10^{-3}	0.59×10^{-3}	M_{R_1} (GeV)	1.4×10^{4}	4.2×10^{4}
r_2	0.59	0.54	M_{R_2} (GeV)	2.9×10^{9}	3.0×10^{9}
δ	261.3°	157.5°	M_{R_3} (GeV)	1.17×10^{11}	3.2×10^{10}
y_ν	0.584	0.66	–	–	–
θ_1	44.3°	115°	θ_{12}	31.5°	33.4°
θ_2	352°	356°	θ_{23}	38.7°	38.8°
θ_3	68.2°	296°	θ_{13}	3.5°	7.41°
m_1 (eV)	1.76×10^{-3}	5.57×10^{-3}	m_1 (eV)	4.6×10^{-4}	4.23×10^{-3}
Δm^2_{12} (eV^2)	5.2×10^{-7}	4.3×10^{-7}	Δm^2_{12} (eV^2)	7.95×10^{-5}	7.38×10^{-5}
Δm^2_{13} (eV^2)	3.2×10^{-3}	3.45×10^{-3}	Δm^2_{13} (eV^2)	2.64×10^{-3}	2.28×10^{-3}
φ_1	0°	253.2°	φ_1	315°	230.2°
φ_2	0°	295.3°	φ_2	295°	235.9°
–	–	–	J_{CP}	-0.56×10^{-2}	−0.0233
–	–	–	M_{ee} (eV)	2.6×10^{-3}	4.3×10^{-3}

with small $\tan\beta$. For large $\tan\beta$ however, there can be significant contribution below the lowest seesaw scale in the MSSM. Some of these mixing scenarios are studied in [23] at high scale without fully considering the effects of Majorana CP phases. In that case our results are somewhat similar and $\theta_{13} < 5°$ is obtained at low energy. The Majorana phases, however, play a significant role in the running of parameters. When non zero value of Majorana phases are considered at the high scale, it is possible to enhance θ_{13} to its allowed 3σ range in the MSSM. Here, we presented a comprehensive study by considering four different mixing scenarios at the GUT scale and study their running behavior in the SM and MSSM with $\tan\beta = 10$. We conclude that for TBM, BM, HM and GR mixings at some high scale, say the GUT scale, the RGE and seesaw threshold

Table 9
Numerical values of input and output parameters radiatively generated in the MSSM for HM mixing for zero and non-zero Majorana phases at $\Lambda_{GUT} = 2 \times 10^{16}$ GeV and $\tan\beta = 10$. The input values for neutrino mixing angles at GUT scale are $\theta_{13} = 0^\circ$, $\theta_{23} = 45^\circ$ and $\theta_{12} = 30^\circ$.

MSSM input	$\varphi_1, \varphi_2 = 0$	$\varphi_1, \varphi_2 \neq 0$	MSSM output	$\varphi_1, \varphi_2 = 0$	$\varphi_1, \varphi_2 \neq 0$
r_1	0.51×10^{-3}	0.68×10^{-3}	M_{R_1} (GeV)	4.36×10^{4}	5.2×10^{4}
r_2	0.49	0.46	M_{R_2} (GeV)	2.2×10^{9}	2.6×10^{9}
δ	34.7°	214.3°	M_{R_3} (GeV)	9.5×10^{10}	3.3×10^{10}
y_ν	0.57	0.675	–	–	–
θ_1	126°	55.6°	θ_{12}	33.8°	35.5°
θ_2	276°	145°	θ_{23}	39.7°	39.9°
θ_3	319°	278.4°	θ_{13}	3.7°	7.3°
m_1 (eV)	2.03×10^{-3}	5.5×10^{-3}	m_1 (eV)	5.84×10^{-4}	3.95×10^{-3}
Δm^2_{12} (eV^2)	4.8×10^{-8}	4.7×10^{-8}	Δm^2_{12} (eV^2)	7.45×10^{-5}	7.6×10^{-5}
Δm^2_{13} (eV^2)	3.0×10^{-3}	3.25×10^{-3}	Δm^2_{13} (eV^2)	2.6×10^{-3}	2.5×10^{-3}
φ_1	0°	304.6°	φ_1	71°	321.4°
φ_2	0°	308.3°	φ_2	99°	322.2°
–	–	–	J_{CP}	0.9×10^{-2}	-0.01
–	–	–	M_{ee} (eV)	2.5×10^{-3}	5.2×10^{-3}

Table 10
Numerical values of input and output parameters radiatively generated in the MSSM for GR mixing for zero and non-zero Majorana phases at $\Lambda_{\rm GUT} = 2 \times 10^{16}$ GeV and $\tan\beta = 10$. The input values for neutrino mixing angles at GUT scale are $\theta_{13} = 0^\circ$, $\theta_{23} = 45^\circ$ and $\theta_{12} = 31.7^\circ$.

MSSM input	$\varphi_1, \varphi_2 = 0$	$\varphi_1, \varphi_2 \neq 0$	MSSM output	$\varphi_1, \varphi_2 = 0$	$\varphi_1, \varphi_2 \neq 0$
r_1	0.58×10^{-3}	0.5×10^{-3}	M_{R_1} (GeV)	7.4×10^{4}	3.87×10^{4}
r_2	0.68	0.53	M_{R_2} (GeV)	4.6×10^{9}	3.6×10^{9}
δ	349.5°	235.5°	M_{R_3} (GeV)	1.36×10^{11}	3.8×10^{10}
y_ν	0.67	0.7	–	–	–
θ_1	242.4°	169°	θ_{12}	35.3°	34.8°
θ_2	116.3°	233.2°	θ_{23}	39.1°	41.3°
θ_3	105°	46.2°	θ_{13}	3.7°	8°
m_1 (eV)	2.1×10^{-3}	4.7×10^{-3}	m_1 (eV)	6.5×10^{-4}	2.8×10^{-3}
Δm^2_{12} (eV^2)	8.8×10^{-7}	4.7×10^{-7}	Δm^2_{12} (eV^2)	7.05×10^{-5}	7.2×10^{-5}
Δm^2_{13} (eV^2)	3.15×10^{-3}	3.0×10^{-3}	Δm^2_{13} (eV^2)	2.47×10^{-3}	2.6×10^{-3}
φ_1	0°	161.2°	φ_1	319.5°	230°
φ_2	0°	325°	φ_2	302.7°	92.8°
–	–	–	J_{CP}	-5.6×10^{-3}	0.012
–	–	–	M_{ee} (eV)	3.0×10^{-3}	2.6×10^{-3}

corrections can result in significant corrections to the mixing angles both in the SM and MSSM at the low energy scale. In the MSSM with $\tan\beta = 10$ it is possible to simultaneously obtain all neutrino mixing angles and mass squared differences in their present 3σ ranges at the EW scale when the Majorana phases are considered. Finally we note that the input values of M_{R_1} taken in our numerical analysis are too small to achieve the successful leptogenesis via the decay of the lightest heavy Majorana neutrino, so a variation of the leptogenesis is required, which is beyond the scope of this work.

Acknowledgements

The work is supported by the National Research Foundation of Korea (NRF) grant funded by Korea Government of the Ministry of Education, Science and Technology (MEST) (Grant No. 2011-0017430, Grant No. 2011-0020333 and Grant No. 2014R1A1A2057665).

References

[1] G. Altarelli, F. Feruglio, Rev. Mod. Phys. 82 (2010) 2701, arXiv:1002.0211 [hep-ph];
H. Ishimori, T. Kobayashi, H. Ohki, H. Okada, Y. Shimizu, M. Tanimoto, Prog. Theor. Phys. Suppl. 183 (2010) 1, arXiv:1003.3552 [hep-th];
S.F. King, C. Luhn, Rep. Prog. Phys. 76 (2013) 056201, arXiv:1301.1340 [hep-ph].
[2] L.L. Everett, A.J. Stuart, Phys. Rev. D 79 (2009) 085005, arXiv:0812.1057 [hep-ph];
F. Feruglio, A. Paris, J. High Energy Phys. 1103 (2011) 101, arXiv:1101.0393 [hep-ph];
G.-J. Ding, L.L. Everett, A.J. Stuart, Nucl. Phys. B 857 (2012) 219, arXiv:1110.1688 [hep-ph];
I.K. Cooper, S.F. King, A.J. Stuart, arXiv:1212.1066 [hep-ph].
[3] F.P. An, et al., DAYA-BAY Collaboration, Phys. Rev. Lett. 108 (2012) 171803, arXiv:1203.1669 [hep-ex];
J.K. Ahn, et al., RENO Collaboration, Phys. Rev. Lett. 108 (2012) 191802, arXiv:1204.0626 [hep-ex];
Y. Abe, et al., DOUBLE-CHOOZ Collaboration, Phys. Rev. Lett. 108 (2012) 131801, arXiv:1112.6353 [hep-ex];
K. Abe, et al., T2K Collaboration, Phys. Rev. Lett. 107 (2011) 041801, arXiv:1106.2822 [hep-ex];
P. Adamson, et al., MINOS Collaboration, Phys. Rev. Lett. 107 (2011) 181802, arXiv:1108.0015 [hep-ex].
[4] C. Jarlskog, Phys. Rev. Lett. 55 (1985) 1039.
[5] G.L. Fogli, E. Lisi, A. Marrone, D. Montanino, A. Palazzo, A.M. Rotunno, Phys. Rev. D 86 (2012) 013012, arXiv:1205.5254 [hep-ph].
[6] D.V. Forero, M. Tortola, J.W.F. Valle, Phys. Rev. D 86 (2012) 073012, arXiv:1205.4018 [hep-ph].
[7] M.C. Gonzalez-Garcia, M. Maltoni, J. Salvado, T. Schwetz, J. High Energy Phys. 1212 (2012) 123, arXiv:1209.3023 [hep-ph].
[8] P.A.R. Ade, et al., Planck Collaboration, arXiv:astro-ph.CO/1303.5076.
[9] P.F. Harrison, D.H. Perkins, W.G. Scott, Phys. Lett. B 530 (2002) 167, arXiv:hep-ph/0202074;
P.F. Harrison, W.G. Scott, Phys. Lett. B 535 (2002) 163, arXiv:hep-ph/0203209;
Zhi zhong Xing, Phys. Lett. B 533 (2002) 85, arXiv:hep-ph/0204049.
[10] F. Vissani, arXiv:hep-ph/9708483;
V.D. Barger, S. Pakvasa, T.J. Weiler, K. Whisnant, Phys. Lett. B 437 (1998) 107, arXiv:hep-ph/9806387;
A.J. Baltz, A.S. Goldhaber, M. Goldhaber, Phys. Rev. Lett. 81 (1998) 5730, arXiv:hep-ph/9806540.
[11] C.H. Albright, A. Dueck, W. Rodejohann, Eur. Phys. J. C 70 (2010) 1099, arXiv:1004.2798 [hep-ph].
[12] A. Datta, F.-S. Ling, P. Ramond, Nucl. Phys. B 671 (2003) 383, arXiv:hep-ph/0306002;
Q. Duret, B. Machet, arXiv:0705.1237 [hep-ph];
Y. Kajiyama, M. Raidal, A. Strumia, Phys. Rev. D 76 (2007) 117301, arXiv:0705.4559 [hep-ph].
[13] C.I. Low, R.R. Volkas, Phys. Rev. D 68 (2003) 033007, arXiv:hep-ph/0305243;
C.S. Lam, Phys. Rev. D 74 (2006) 113004, arXiv:hep-ph/0611017.
[14] Z.-z. Xing, Phys. Lett. B 533 (2002) 85, arXiv:hep-ph/0204049;
S.K. Kang, Z.z. Xing, S. Zhou, Phys. Rev. D 73 (2006) 013001, arXiv:hep-ph/0511157;
R.N. Mohapatra, W. Rodejohann, Phys. Rev. D 72 (2005) 053001, arXiv:hep-ph/0507312;
S. Antusch, S.F. King, Phys. Lett. B 631 (2005) 42, arXiv:hep-ph/0508044;
S.K. Kang, C.S. Kim, Phys. Lett. B 634 (2006) 520, arXiv:hep-ph/0511106;
S. Boudjemaa, S.F. King, Phys. Rev. D 79 (2009) 033001, arXiv:0808.2782 [hep-ph];
Y. Shimizu, R. Takahashi, Europhys. Lett. 93 (2011) 61001, arXiv:1009.5504 [hep-ph];
D. Meloni, F. Plentinger, W. Winter, Phys. Lett. B 699 (2011) 354, arXiv:1012.1618 [hep-ph];
Y.-j. Zheng, B.-Q. Ma, Eur. Phys. J. Plus 127 (2012) 7, arXiv:1106.4040 [hep-ph];
Z.-Z. Xing, Chin. Phys. C 36 (2012) 101, arXiv:1106.3244 [hep-ph];
T. Araki, Phys. Rev. D 84 (2011) 037301, arXiv:1106.5211 [hep-ph];
S. Dev, S. Gupta, R.R. Gautam, Phys. Lett. B 704 (2011) 527, arXiv:1107.1125 [hep-ph];
S.K. Kang, C.S. Kim, Phys. Rev. D 90 (2014) 077301, arXiv:1406.5014 [hep-ph];
S. Gupta, C.S. Kim, Pankaj Sharma, Phys. Lett. B 740 (2015) 353, arXiv:1408.0172 [hep-ph].

[15] T. Miura, T. Shindou, E. Takasugi, Phys. Rev. D 68 (2003) 093009, arXiv:hep-ph/0308109;
S. Luo, Z.z. Xing, Phys. Lett. B 632 (2006) 341, arXiv:hep-ph/0509065;
S. Luo, Z.-z. Xing, Phys. Lett. B 637 (2006) 279, arXiv:hep-ph/0603091;
S. Luo, Z.-z. Xing, Phys. Lett. B 632 (2006) 341, arXiv:hep-ph/0509065;
A. Dighe, S. Goswami, W. Rodejohann, Phys. Rev. D 75 (2007) 073023, arXiv:hep-ph/0612328;
A. Dighe, S. Goswami, P. Roy, Phys. Rev. D 76 (2007) 096005, arXiv:0704.3735 [hep-ph];
S. Luo, Z.-z. Xing, Phys. Rev. D 86 (2012) 073003, arXiv:1203.3118 [hep-ph].
[16] S. Luo, Z.z. Xing, Phys. Rev. D 86 (2012) 073003, arXiv:1203.3118 [hep-ph];
T. Ohlsson, H. Zhang, S. Zhou, Phys. Rev. D 87 (2013) 013012, arXiv:1211.3153 [hep-ph].
[17] S. Ray, Int. J. Mod. Phys. A 25 (2010) 4339, arXiv:1005.1938 [hep-ph];
T. Ohlsson, S. Zhou, arXiv:1311.3846 [hep-ph].
[18] P. Minkowski, Phys. Lett. B 67 (1977) 421;
T. Yanagida, in: O. Sawada, A. Sugamoto (Eds.), Proceedings of the Workshop on the Unified Theory and the Baryon Number in the Universe, KEK, Tsukuba, Japan, 1979, p. 95;
M. Gell-Mann, P. Ramond, R. Slansky, Complex Spinors and Unified Theories, in: P. Van Nieuwenhuizen, D.Z. Freedman (Eds.), Supergravity, North-Holland, Amsterdam, 1979, p. 315;
R.N. Mohapatra, G. Senjanovic, Phys. Rev. Lett. 44 (1980) 912.
[19] P.H. Chankowski, Z. Pluciennik, Phys. Lett. B 316 (1993) 312, arXiv:hep-ph/9306333;
K.S. Babu, C.N. Leung, J.T. Pantaleone, Phys. Lett. B 319 (1993) 191, arXiv:hep-ph/9309223;
J.A. Casas, J.R. Espinosa, A. Ibarra, I. Navarro, Nucl. Phys. B 573 (2000) 652, arXiv:hep-ph/9910420;
J.A. Casas, J.R. Espinosa, A. Ibarra, I. Navarro, Nucl. Phys. B 569 (2000) 82, arXiv:hep-ph/9905381;
A.S. Joshipura, S.D. Rindani, N.N. Singh, Nucl. Phys. B 660 (2003) 362, arXiv:hep-ph/0211378.
[20] S. Antusch, M. Drees, J. Kersten, M. Lindner, M. Ratz, Phys. Lett. B 519 (2001) 238, arXiv:hep-ph/0108005;
S. Antusch, M. Drees, J. Kersten, M. Lindner, M. Ratz, Phys. Lett. B 525 (2002) 130, arXiv:hep-ph/0110366;
S. Antusch, J. Kersten, M. Lindner, M. Ratz, Phys. Lett. B 538 (2002) 87, arXiv:hep-ph/0203233.
[21] S. Antusch, J. Kersten, M. Lindner, M. Ratz, Nucl. Phys. B 674 (2003) 401, arXiv:hep-ph/0305273;
A. Dighe, S. Goswami, S. Ray, Phys. Rev. D 79 (2009) 076006, arXiv:0704.3735 [hep-ph].
[22] S. Antusch, J. Kersten, M. Lindner, M. Ratz, M.A. Schmidt, J. High Energy Phys. 0503 (2005) 024, arXiv:hep-ph/0501272.
[23] J.-w. Mei, Z.-z. Xing, Phys. Rev. D 70 (2004) 053002, arXiv:hep-ph/0404081.
[24] J. Bergstrom, M. Malinsky, T. Ohlsson, H. Zhang, Phys. Rev. D 81 (2010) 116006, arXiv:1004.4628 [hep-ph];
J. Bergstrom, T. Ohlsson, H. Zhang, Phys. Lett. B 698 (2011) 297, arXiv:1009.2762 [hep-ph];
J.-w. Mei, Phys. Rev. D 71 (2005) 073012, arXiv:hep-ph/0502015.
[25] W. Grimus, L. Lavoura, Eur. Phys. J. C 39 (2005) 219, arXiv:hep-ph/0409231.
[26] J.R. Ellis, S. Lola, Phys. Lett. B 458 (1999) 310, arXiv:hep-ph/9904279.
[27] P.H. Chankowski, S. Pokorski, Int. J. Mod. Phys. A 17 (2002) 575, arXiv:hep-ph/0110249.
[28] S. Goswami, S. Khan, S. Mishra, Int. J. Mod. Phys. A 29 (2014) 1450114, arXiv:1310.1468 [hep-ph].
[29] N. Haba, Y. Matsui, N. Okamura, Eur. Phys. J. C 17 (2000) 513, arXiv:hep-ph/0005075.
[30] J.A. Casas, J.R. Espinosa, A. Ibarra, I. Navarro, Nucl. Phys. B 573 (2000) 652, arXiv:hep-ph/9910420.
[31] M. Auger, et al., EXO Collaboration, Phys. Rev. Lett. 109 (2012) 032505, arXiv:1205.5608 [hep-ex].
[32] A. Gando, et al., KamLAND-Zen Collaboration, Phys. Rev. Lett. 110 (2013) 6, 062502, arXiv:1211.3863 [hep-ex].